3.7 Developing a Method for Resolving NOx Emission Inventory Biases Using Discrete Kalman Filter Inversion, Direct Sensitivities, and Satellite-Based NO_2 Columns

Sergey L. Napelenok, Robert W. Pinder, Alice B. Gilliland and Randall V. Marin

Abstract An inverse method was developed to integrate satellite observations of atmospheric pollutant column concentrations with specie concentrations and direct sensitivities predicted by a regional air quality model in order to discern biases in the emissions of the pollutant precursors. Using this method, the emission fields were analyzed using a "top-down" approach with an inversion performed by Discrete Kalman Filter (DKF) and direct sensitivities calculated using the Decoupled Direct Method in 3D (DDM-3D) embedded in the Community Multiscale Air Quality (CMAQ) model. The system was tested through an experiment focusing on NO_2 concentrations and emissions of NOx in the southeastern United States. The method reproduced the expected NOx emission fields from initially perturbed starting values. Responses to different parameters in the system, including assumptions for uncertainties in the emission fields and satellite observations, were also tested. The method is readily extendable to other pollutants.

Keywords DDM-3D, direct decoupled method, emissions, inverse modeling, Kalman filter, satellite, sensitivity, NO_2, NOx,

1. Introduction

Current regional air quality models rely on well-developed emission inventories with high spatial and temporal resolution. While much work has been done in the development of such inventories, uncertainties still exist. At the same time, retrieval techniques for satellite data have improved and several datasets are available for observations of NO_2, CO, and some hydrocarbons recorded by several satellites in orbit.

A method was developed for using satellite NO_2 column observations to check for biases in current emission inventories of NOx with Discrete Kalman filter (DKF) inversion and sensitivities calculated by the Decoupled Direct Method in three dimensions (DDM-3D), which had been previously integrated (Cohan et al.,

C. Borrego and A.I. Miranda (eds.), *Air Pollution Modeling and Its Application XIX.*

2005; Napelenok et al., 2006) into the Community Multiscale Air Quality (CMAQ) model (Byun and Schere, 2006). The method was tested using a pseudodata scenario representing hypothetical satellite observations. A base-case CMAQ simulation acted as the true representation of the relationship between NOx emissions and NO_2 column concentrations in the domain. Ground-level NOx emissions were then adjusted in pre-defined geographic regions within the modeling domain to mimic possible biases. Finally, the inverse procedure was applied to attempt to arrive back at the base-case emissions taking into account uncertainties in transport and chemistry. The method has proved to converge robustly at the correct solution in only a few iterations for various spatially distributed emission biases.

Integration of satellite observations of NO_2 with regional air quality modeling efforts can potentially reduce uncertainty in emission inventories. Retrieval algorithms for NO_2 column densities have been developed for several satellites, including GOME (Richter and Burrows, 2002), SCIAMACHY (Sioris et al., 2004), and more recently, OMI (Bucsela et al., 2006). Inverse modeling of NOx emissions has been applied previously, but typically on a global scale (Martin et al., 2003; Muller and Stavrakou, 2005) with some efforts on a continental scale (Quelo et al., 2005; Konovalov et al., 2006). In finer scale NO_2 inverse modeling, the difficulties arise from the importance of resolving the nonlinearities in chemistry and transport, which are overcome in this exercise with the aid of direct sensitivities.

2. Method

2.1. Discrete Kalman filter

Inverse modeling of the NOx emissions field was performed using Discrete Kalman Filter. DKF is an optimization technique used to estimate discrete time series and states that are governed by sets of linear differential equations. It has seen frequent use in inverse modeling of emissions on both the global scale and regional scales for various gaseous and particulate species (Hartley and Prinn, 1993; Chang et al., 1996; Haas-Laursen et al., 1996; Gilliland et al., 2003). Since chemical transport models also parameterize nonlinear processes, the linearity assumption is overcome by applying DKF iteratively. This method is also attractive for inverse modeling, because it allows for the use of uncertainty information in both the emissions fields and the observed pollutant values. A brief overview of DKF is presented here, while more detailed explanation is available elsewhere (Gilliland and Abbitt, 2001).

DKF evolves the emission vector, $\overline{E}_t$, according to the following:

$$\overline{E}_{t,k+1} = \overline{E}_{t,k} + \mathbf{G}_{t,k}\left(\overline{\chi}_t^{obs} - \overline{\chi}_t^{\mathrm{mod}}\right) \quad (1)$$

At iteration $k+1$ and time t, the emissions vector is altered based on the gain matrix, $\mathbf{G}_{t,k}$, and the difference between the vectors of observations, $\overline{\chi}_t^{obs}$, and

modeled values, $\overline{\chi}_t^{mod}$. The gain matrix is defined in terms of the matrix of partial derivatives of the change in concentration with respect to emissions, $\mathbf{P}_t$, the matrix of the covariance of the error in the emissions field, $\mathbf{C}_{t,k}$, and the noise matrix, $\mathbf{N}_t$, such that:

$$\mathbf{G}_{t,k} = \mathbf{C}_{t,k}\mathbf{P}_t^T\left(\mathbf{P}_t\mathbf{C}_{t,k}\mathbf{P}_t^T + \mathbf{N}_t\right)^{-1} \quad (2)$$

The covariance of error matrix also evolves with subsequent iterations according to:

$$\mathbf{C}_{t,k+1} = \mathbf{C}_{t,k} - \mathbf{G}_{t,k}\mathbf{P}_t\mathbf{C}_{t,k} \quad (3)$$

The covariance functionally determines the degree to which the emissions vector is allowed to deviate from its initial values. As iterations are progressed, the covariance is reduced according to Eq. (3) and subsequent differences between $\overline{E}_{t,k+1}$ and $\overline{E}_{t,k}$ are smaller in a mathematically stable system. In this application, the initial covariance of the error in the integrated emissions estimates, $\mathbf{C}_{t,k=0}$, was based on an estimate of the normalized uncertainty in the emissions, U_E, according to the following:

$$C_{jj} = \left(U_{E,j} \cdot E_j\right)^2 \quad (4a)$$

$$C_{jk,j\neq k} = \left(0.1 \cdot \frac{U_{E,j} + U_{E,k}}{2} \cdot \frac{E_j + E_k}{2}\right)^2 \quad (4b)$$

Similarly, the noise matrix was based on the estimated normalized uncertainties in the observations, U_{obs}, according to:

$$N_{jj} = Max\left[0.5, \left(U_{obs,j} \cdot \chi_{j,t}^{obs}\right)^2\right] \quad (5a)$$

$$N_{jk,j\neq k} = 0.0 \quad (5b)$$

Theoretically, the noise matrix, $\mathbf{N}_t$, can account for both errors in observations, as it does here, and also errors in the modeling system. The minimum value of 0.5 (10^{15} molecules/cm^2)^2 was imposed to prevent mathematical instability.

2.2. Decoupled direct method in 3D

The relationship between precursor emissions and resulting pollutant concentrations was represented using sensitivities calculated using the Decoupled Direct Method in 3D. DDM-3D is an efficient and convenient way to calculate responses in the outputs of an air quality model to perturbations in various combinations of input parameters (Dunker, 1981; Yang et al., 1997). DDM-3D propagates sensitivities using some of the same algorithms that are in place to solve the atomspheric diffusion equation:

$$\frac{\partial C_i}{\partial t} = -\nabla\left(uC_i\right) + \nabla\left(K\nabla C_i\right) + R_i + E_i \quad , \quad (6)$$

where C_i is the concentration of species i, u is the fluid velocity, K is the diffusivity tensor, R is rate of chemical generation, and E is the emissions field. An analogous equation is developed to calculate sensitivities:

$$\frac{\partial S_{ij}}{\partial t} = -\nabla\left(uS_{ij}\right) + \nabla\left(K\nabla S_{ij}\right) + J_i S_{ij} + E_i^{'}, \tag{7}$$

where J_i is the ith row vector in the Jacobian matrix J, which represents the chemical interactions between species ($J_{ij} = \partial R_i / \partial C_j$), and S_i is defined as the change of a pollutant i in space, $\bar{x}$, and time, t, in respect to a perturbation in some model parameter, (emission rate, initial condition, etc.):

$$S_{ij}\left(\bar{x},t\right) = \frac{\partial C_i\left(\bar{x},t\right)}{\partial p_j}. \tag{8}$$

Implementation of DDM-3D for the CMAQ model has been evaluated previously for both gaseous and particulate species and has been shown be suitable for producing NO_2 sensitivities to NOx emissions as compared to discrete difference sensitivity methods (Cohan et al., 2005; Napelenok et al., 2006).

3. Pseudodata Analysis

To evaluate the inverse modeling system, a pseudodata scenario was developed in a sample domain centered on the southeastern United States. Emissions source regions were defined based on similar spatial emissions patterns of ground-level NOx during the summer months of 2004 and included the urban areas of Memphis, TN; Nashville, TN; Birmingham, AL; Atlanta, GA; and Macon, GA, as well as the rural areas approximately covered by the states of Tennessee, Mississippi, Alabama, and Georgia (Figure 1). A 144 km wide margin was left around the source regions in order to completely resolve sensitivity fields originating from the defined regions.

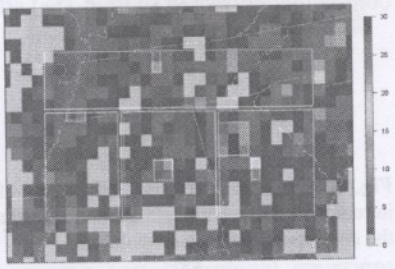

Fig. 1 Source region definitions and average ground-level hourly NOx emissions (moles/s) on August 1, 2004

CMAQ with DDM-3D simulated base concentration fields of NO_2 and sensitivities to NOx emissions from each source region. Sensitivities to the emissions from the surrounding "border" region and to the boundary conditions were also

calculated and were found to have negligible impact on NO_2 column densities in the inner region (Figure 2).

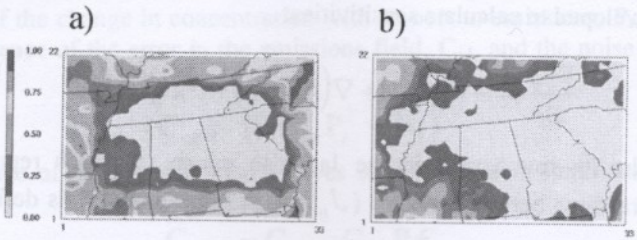

Fig. 2 Fractional contribution of total NO_2 column sensitivity to NOx emissions only from (a) 144 km "border" region and (b) boundary conditions. The total NO_2 column sensitivity is the sum of sensitivities to each source in addition to (a) and (b)

The emission rates in each source region were then arbitrarily adjusted by factors ranging between 0.6 and 1.7 and the simulation repeated with the assumption that the emissions were homogeneous within the region. NO_2 concentrations and sensitivities from each simulation were aggregated to column values to more closely mimic the type of available satellite data. The perturbed emissions vector and the corresponding gridded NO_2 column values became the *a priori* estimate for the inverse method ($\overline{E}_t$ and $\overline{\chi}_t^{\text{mod}}$), while the base-case NO_2 columns were used as the representation of the "truth" in the inverse ($\overline{\chi}_t^{obs}$). DKF was then applied iteratively, recalculating concentration and sensitivity fields for each k.

During this exercise, the uncertainties in the emissions were set to be relatively high (U_E = 2.0) to allow a large range of deviation from the *a priori* emissions vector in the subsequent estimations. The uncertainty in observations was set low (U_{obs} = 0.1) to allow the modeled values to closely approach the observations. This combination of uncertainty parameters allows for the best test of the robustness of the system at arriving at the correct solution.

The application of this pseudodata scenario revealed that the proposed inverse method was able to reproduce the original base-case emissions vector within only a few iterations (Figure 3). The corresponding NO_2 fields were also nearly completely corrected (within 1%) after just four iterations (Fig.).

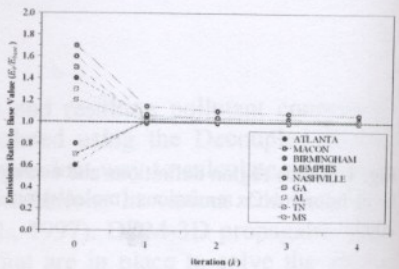

Fig. 3 Aggregated regional emissions after each iteration in the pseudodata scenario normalized by the corresponding base-case values

Developing a Method for Res

Fig. 4 Comparison of expec- ted and modeled NO_2 column values in each grid cell fo (a) initial perturbed simula- tion and (b) the result of th inverse after four iteration (all values in 10^{15} molecule cm^{-2})

The response of the sy analyzing the predicted (k = 1). In this pseudoda after the first iteration further for this analysis lead to larger values in the emissions fields, w allow for larger adjustm of error matrix $C_{t,k=0}$ measurements from the approximately 0.5 × 1 retrieval algorithms (M the lower end of the t emissions uncertainties there are no mathemati a solution in fewer itera

Fig. 5 Regional emission iteration normalized by the case values as a function of vations and uncertainties in show immediate near per perturbations are noted nex

4. Discussion

The proposed method values in the pseudoda is likely to be more co retrieval is not disrup to penetrate, the geog

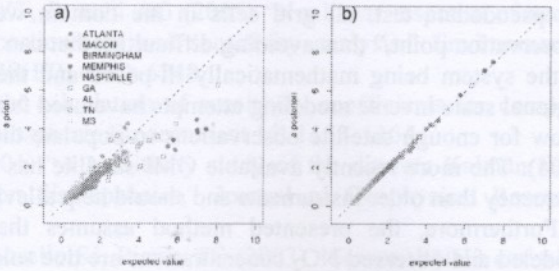

Fig. 4 Comparison of expected and modeled NO_2 column values in each grid cell for (a) initial perturbed simulation and (b) the result of the inverse after four iterations (all values in 10^{15} molecules cm^{-2})

The response of the system to uncertainty assumptions was also evaluated by analyzing the predicted regional emissions adjustment after the first DKF iteration ($k = 1$). In this pseudodata scenario, the acceptable solution was found immediately after the first iteration (Figure 1); thus it was not necessary to carry the solution further for this analysis. As expected, large uncertainties in the observations that lead to larger values in the noise matrix (N_t) do not allow for large adjustments to the emissions fields, while large uncertainties in the *a priori* emissions estimates allow for larger adjustments through increasing the values in the initial covariance of error matrix $C_{t,k=0}$ (Figure 5). Actual uncertainties in the NO_2 column density measurements from the SCIAMACHY and GOME satellite have been shown to be approximately 0.5×10^{15} molecules cm^{-2} +30% from various assumptions in the retrieval algorithms (Martin et al., 2002; Boersma et al., 2004) suggesting values at the lower end of the tested range. It is more difficult to arrive at estimates of emissions uncertainties in specific geographic regions, but it was shown that if there are no mathematical instabilities, larger values should be selected to arrive at a solution in fewer iterations.

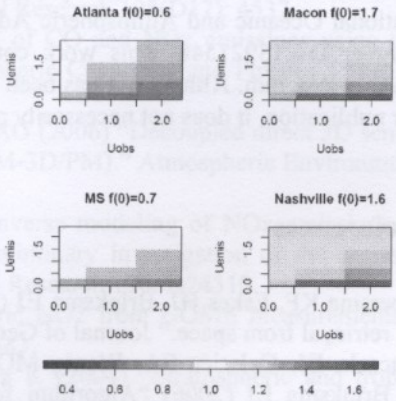

Fig. 5 Regional emissions after the first DKF iteration normalized by their corresponding base-case values as a function of uncertainties in observations and uncertainties in emissions. White areas show immediate near perfect prediction. Initial perturbations are noted next to region names

4. Discussion

The proposed method was successful at reproducing correct regional emissions values in the pseudodata exercise. The translation to actual satellite measurements is likely to be more complex due to the limited coverage of the observations. When retrieval is not disrupted by heavy cloud cover that the instruments are unable to penetrate, the geographical extent of what is observed is relatively small. In

the pseudodata test, all grid cells in the domain were allowed to represent an "observation point," thus avoiding difficulties that can arise with real data resulting in the system being mathematically ill-posed and therefore unconstrained. Other regional scale inverse modeling attempts have used fairly long averaging periods to allow for enough satellite observations to populate the domain (Konovalov et al., 2006). The more recently available OMI satellite has significantly better overpass frequency than older instruments and should help alleviate this problem.

Furthermore, the presented method assumes that the discrepancies in the modeled and observed NO_2 concentrations are due solely to estimates of emissions at the ground level. Uncertainties in the chemical processes, emissions aloft from lightning sources and airplanes, and meteorological predictions also contribute to differences between modeled concentrations of NO_2 and satellite observations. These uncertainties should be quantified and included in the noise matrix. The presented pseudodata analysis tests the reliability of the method before adding these complexities.

Overall, the method is computationally efficient due to the ability to calculate sensitivities directly using DDM-3D and the fact that the matrix operations required by DKF are computationally insignificant. It promises to be directly applicable to NOx emissions inventory analysis and extendable to other species.

Acknowledgments The authors would like to thank for contributions and advice from Rynda Hudman and Robin Dennis and insightful comments from all reviewers. Work at Dalhousie University was supported by the Natural Sciences and Engineering Research Council of Canada. A portion of the research presented here was performed under the Memorandum of Understanding between the U.S. Environmental Protection Agency (EPA) and the U.S. Department of Commerce's National Oceanic and Atmospheric Administration (NOAA) and under agreement number DW13921548. This work constitutes a contribution to the NOAA Air Quality Program. Although it has been reviewed by EPA and NOAA and approved for publication, it does not necessarily reflect their policies or views.

References

Boersma KF, Eskes HJ, Brinksma EJ (2004) "Error analysis for tropospheric NO2 retrieval from space." Journal of Geophysical Research 109: D04311.

Bucsela EJ, Celarier EA, Wenig MO, Gleason JF, Veefkind JP, Boersma KF, Brinksma EJ (2006) "Algorithm for NO_2 vertical column retrieval from the ozone monitoring instrument." IEEE Transactions on Geoscience and Remote Sensing 44(5): 1245–1258.

Byun DW, Schere KL (2006) "Review of the governing equations, computational algorithms, and other components of the Models-3 Community Multiscale Air Quality (CMAQ) modeling system." Applied Mechanics Reviews 59: 51–77.

Chang ME, Hartley DE, Cardelino C, Chang W-L (1996) "Inverse modeling of biogenic isoprene emissions." Geophysical Research Letters 23: 3007–3010.

Cohan DS, Hakami A, Hu YT, Russell AG (2005) "Nonlinear response of ozone to emissions: source apportionment and sensitivity analysis." Environmental Science and Technology 39(17): 6739–6748.

Dunker AM (1981) "Efficient calculation of sensitivity coefficients for complex atmospheric models." Atmospheric Environment 15: 1155–1161.

Gilliland AB, Abbitt PJ (2001) "A sensitivity study of the discrete Kalman filter (DKF) to initial condition discrepancies." Journal of Geophysical Research 106(D16): 17939–17952.

Gilliland AB, Dennis RL, Roselle SJ, Pierce TE (2003) "Seasonal NH3 emission estimates for the eastern United States based on ammonium wet concentrations and an inverse method." Journal of Geophysical Research 108(D15): 4477.

Haas-Laursen DE, Hartley DE, Prinn RG (1996) "Optimizing an inverse method to deduce time-varying emissions of trace gases." Journal of Geophysical Research 101(D17): 22823–22831.

Hartley DE, Prinn RG (1993) "Feasibility of determining surface emissions of trace gases using an inverse method in a three-dimensional chemical transport model." Journal of Geophysical Research 98: 5183–5197.

Konovalov IB, Beekmann M, Richter A, Burrows JP (2006) "Inverse modelling of the spatial distribution of NOx emissions on a continental scale using satellite data." Atmospheric Chemistry and Physics 6: 1747–1770.

Martin RV, Chance K, Jacob DJ, Kurosu TP, Spurr RJD, Bucsela E, Gleason JF, Palmer PI, Bey I, Fiore AM, Li Q, Yantosca RM, Koelemeijer RBA (2002) "An improved retrieval of tropospheric nitrogen dioxide from GOME." Journal of Geophysical Research 107: 4437.

Martin RV, Jacob DJ, Chance K, Kurosu TP, Palmer, Evans MJ (2003) "Global inventory of nitrogen oxide emissions constrained by space-based observations of NO2 columns." Journal of Geophysical Research 108(D17): 4537.

Muller J-F, Stavrakou T (2005) "Inversion of CO and NOx emissions using the adjoint of the IMAGES model." Atmospheric Chemistry and Physics 5: 1157–1186.

Napelenok SL, Cohan DS, Hu YT, Russell AG (2006) "Decoupled direct 3D sensitivity analysis for particulate matter (DDM-3D/PM)." Atmospheric Environment 40(32): 6112–6121.

Quelo D, Mallet V, Sportisse B (2005) "Inverse modeling of NOx emissions at regional scale over northern France: preliminary investigation of the second-order sensitivity." Journal of Geophysical Research 110: D24310.

Richter A, Burrows JP (2002) "Tropospheric NO2 from GOME measurements." Advances in Space Research 29: 1673–1683.

Sioris CE, Kurosu TP, Martin RV, Chance K (2004) "Stratospheric and tropospheric NO2 observed by SCIAMACHY: first results." Advances in Space Research 34: 780–785.

Yang YJ, Wilkinson JG, Russell AG (1997) "Fast, direct sensitivity analysis of multidimensional photochemical models." Environmental Science and Technology 31(10): 2859–2868.